Controlling Optical Properties of Complex Emulsions via γ-cyclodextrin Degradation for Colorimetric Sensing Applications

Ashley P. Saunders, McNair Scholar, The Pennsylvania State University

McNair Faculty Research Adviser: Lauren D. Zarzar, Ph.D.
Assistant Professor of Chemistry
Department of Chemistry
Eberly College of Science
The Pennsylvania State University

Abstract

Structural coloration plays an important role in daily phenomena as one of the main mechanisms of color in nature and materials. Complex emulsion droplets consisting of hydrocarbon and fluorocarbon oils have previously been shown to exhibit iridescent structural color via total internal reflection based on the size, shape, composition, and orientation of the droplets.[1] Our study works to further explore the optical properties of complex emulsion droplets and their applications through the use of an enzyme-active surfactant solution composed of α – amylase, γ – cyclodextrin, Triton X – 100 , Capstone FS – 30. We aim to quantize the sensitivity of O/O/W emulsion droplets for colorimetric sensing capabilities and enzyme activity through the correlation of color patterns to droplet shape, size, and volume ratio.

1) Goodling, A. E.; Nagelberg, S.; Kaehr, B.; Meredith, C. H.; Cheon, S. I.; Saunders, A. P.; Kolle, M.; Zarzar, L. D. *Nature* **2019**, *566* (7745).

Introduction

Structural coloration is one of the main modes of color in nature among pigments and bioluminescence. This mode of color arises from micron and nano-structures that are on the same scale as the wavelengths of visible light, which act to diffract or reflect the light impacting them. Structural color is observed in organisms such as peacock feathers,[1] neon tetra fish[2]; in natural phenomena such as glories and rainbows; and in household items such as CDs and DVDs. Goodling et al. have also shown that structural coloration can be caused by monodispersed complex emulsion droplets formed of fluorocarbon and hydrocarbon oils.[3]

Simple oil in water (O/W) emulsions are composed of oil droplets in a larger water continuous phase. The spherical droplets formed are the result of the high interfacial tensions caused by interactions between the two liquids. Without the addition of surface-active agents ("surfactants"), this system would be prone to Ostwald ripening and coalescence. Surfactants act at the interface of substances to lower interfacial tensions between the two phases and allow for the formation of stable emulsion droplets. This provides a gateway to forming more complex systems of O/O/W, W/O/W, etc., which can be made reconfigurable by changing surfactant concentrations.[4]

Goodling et al. utilized reconfigurable hydrocarbon and fluorocarbon double emulsions to generate vibrant colors via the total internal reflection of white light. The total internal reflection mechanism begins with white light impacting the tree way contact point between the two oils and outer water phase. The light then becomes separated according to wavelength as it is reflected at the interface between the two oils and exits at the opposite side of the droplet. Separation of colors depend on the number of reflections that an electromagnetic wave experience. Due to this mechanism, the coloration in these emulsion droplets is heavily reliant on the refractive index match between the two oils, droplet size, shape of the interface between the oils, and the orientation of the droplet.[3]

Enzymes offer remote controllability over these emulsions by continuously changing the curvature of the oil-oil interface. A previous study by Zarzar et al. utilizes interactions between the enzyme α – amylase, the sugar γ-cyclodextrin, and the hydrocarbon surfactant Triton X-100 (TriX), among others, to develop a system that quantifies the enzyme activity.[5] Enzyme responsive surfactant is formed by mixing the Triton X with γ-cyclodextrin, as they form a 1:1 inclusion complex in solution.[6] This complexation process renders the TriX inactive as a surfactant and causes the biphasic O/O/W emulsion droplets to only respond to free fluorosurfactant in solution. The addition of α-amylase causes the degradation of γ-cyclodextrin via hydrolysis, thus freeing the TriX and gradually changing the droplet shape to a hydrocarbon favored phase.[5]

These findings of coloration and enzyme interactions may be combined and utilized to remotely and thoroughly study the continuous impact of droplet shape on the color projection patterns of complex emulsions. It can also give insight into the continuous changing nature of interfacial tensions between the hydrocarbon and fluorocarbon oils and can offer the beginnings of color control in the complex hydrocarbon/fluorocarbon emulsion system. Observation of α-amylase is also useful for the detection of physical and psychological stress in humans and animals.[7,8] For example, alpha-amylase levels that are observed to reach four to six times their reference value (normally 26 – 102 FAU/L in adults) in plasma can be an indication of pancreatitis – inflammation of the pancreas.[9,10]

Methods

Chemicals. All chemicals were used as received. Capstone FS-30 (Cap) and perfluorohexane(s) (SynQuest Laboratories); Triton X-100 and α-amylase from *Aspergillus oryzae* (Product A8220, Batch SLBV4784) (Sigma Aldrich); sodium acetate and hexane(s) (Fisher Scientific); hydrochloric acid, 1N (Ricca Chemical); γ-cyclodextrin (Tokyo Chemical Industry); heptane (VWR International).

Sodium acetate buffer. The sodium acetate buffer solution was formed by adding hydrochloric acid (1N) to an aqueous sodium acetate solution (0.2 M) until the pH of the resultant solution was near a pH of 5.2. The pH was monitored using the Mettler Toledo Seven Compact s220 pH/ion meter. The sodium acetate buffer solution was then used as the standard solution for all subsequent stock solutions of Triton X-100, Capstone FS-30, γ-cycodextrin, and α-amylase.

Droplet fabrication. Biphasic emulsion droplets were fabricated via microfluidics using a 4-inlet 100 micron channel depth hydrophilic glass microfluidics chip (Dolomite). The two inner channels were used for hydrocarbon and fluorocarbon oil flows, while the outermost channels were used for aqueous surfactant flow. Flow channels were connected to reservoirs of desired liquids via 30 inch poly ether ether ketone (PEEK) tubing of inner diameter 0.0025 inches and outer diameter 1/16 inches. Liquid flow within the microfluidics chip was controlled by the Fluigent MFCS-EZ pressure controller. Pressures ranges for the inner and outer channels ranged from 250 – 350 and 2000 – 3000 respectively. Typical inner phases included combinations of heptane, hexane, and perfluorohexane, while combinations of Capstone FS-30, Triton X-100, and γ-cyclodextrin served as common outer phases.

Microscopic Imaging. All transmission photomicrographs were taken with the Nikon Eclipse Ti-U inverted microscope. Droplets orient with the denser fluorocarbon phase downward. To image the side-view of the droplets the containment dish was shaken to induce the droplets to roll onto their side. Then an image was captured with an Image Source DFK 23UX249 color camera. Photomicrographs of droplets in reflection were taken with the Zeiss Axioscope upright reflection microscope at exposures between 5 – 30ms.

Macroscopic Imaging. Samples for macroscopic images or videos were first prepared by filling a 35-mm petri dish lid or 24-well plate with a monolayer of emulsion droplets. All petri dishes and well plates were painted with black acrylic paint to limit reflection from the bottom layer of plastic. For small area illumination, a specific area of the droplets was exposed to a Thorlabs LED light (MWWHF2, 4,000 K, 16.3 mW) fit with a 200 μm-diameter fiber optic cable and collimating lens (CFC-2X-A). For large area illumination, an Amscope LED 50 W light with a collimating lens was used to illuminate the full sample. Images of color projections were collected by placing a hemisphere of a ping-pong ball with a three-millimeter hole in it on top of the sample and illuminating a small area of the sample. Images and videos were collected using a Canon EOS Rebel T6 DSLR camera mounted on an optical table with the light source. Phone images and videos were collected with the Galaxy Note 8 phone camera, and the phone flash was used as the only source of illumination.

Angle measurements seen in text were measured using the optical table or with the Android application Bubble Level (v 3.23) of ±0.1° accuracy. A diagram of ping-pong ball imaging used in this experiment may be observed below in Figure 1.

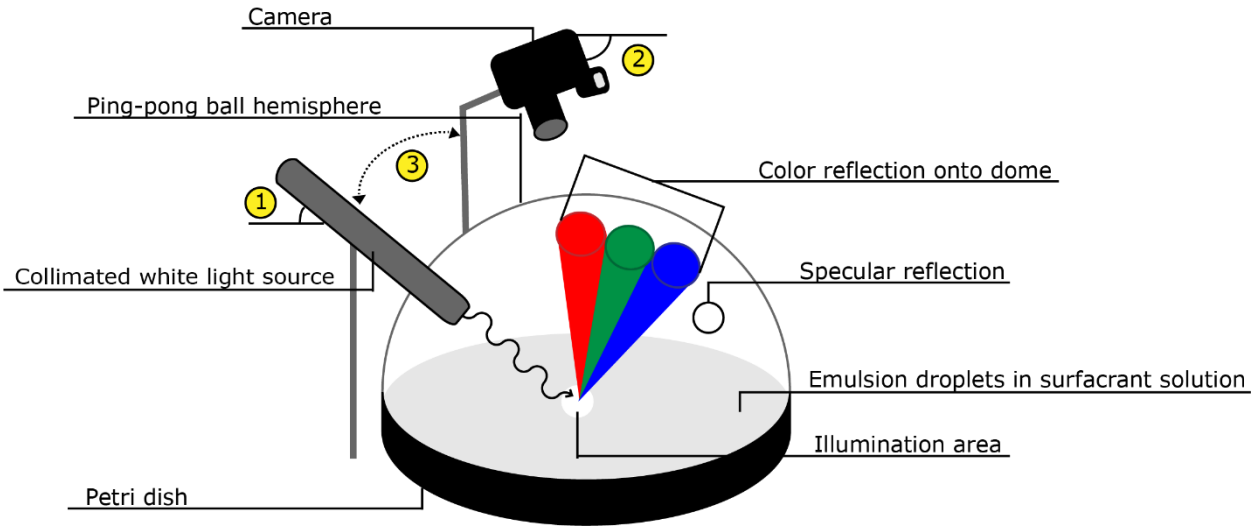

Figure 1. A simplified diagram of the ping-pong ball projection method adapted from Goodling et. al.[3] A ping-pong ball hemisphere is placed on top of a petri dish lid containing emulsion droplets in aqueous surfactant solution. Droplets are illuminated with a white light source and then produce a band of coloration onto the dome. Coloration within the graphic has been limited to the red, green and blue spots for simplification and to prevent obstruction of detailing, as true color order and position patterns vary by droplet shape and size. Numbers 1, 2, and 3 correspond to and define illumination angle (IA), camera angle (CA), and light-to-camera angle (LCA) respectively. Items are not drawn to scale.

α-amylase calibration, detection, and transition. Amylase calibration was conducted by filling two wells of a 24-well plate with one milliliter of 0.2 wt% Capstone FS-30 and then 19 microliters and 24 microliters of 0.2 wt% Triton X-100 to the separate wells. Other wells were filled with one milliliter of 5:1:6 or 5:1:8 ratio by weight of Capstone FS-30: Triton X-100: γ-cyclodextrin (CTγ) with Capstone being 0.2 wt% in concentration for amylase detection or transitions respectively. A monolayer of perfluorohexane (PFH) and 1:1 heptane/hexane by volume emulsion droplets formed via microfluidics was then added to each well. Lastly, detection wells were exposed to 100 microliters of alpha amylase stock solutions ranging from 88.3 - 883 FAU/L and transition wells were exposed to 1 – 5 microliters of 10 wt% amylase stock.

Results and Discussion

Band position as a function of droplet shape

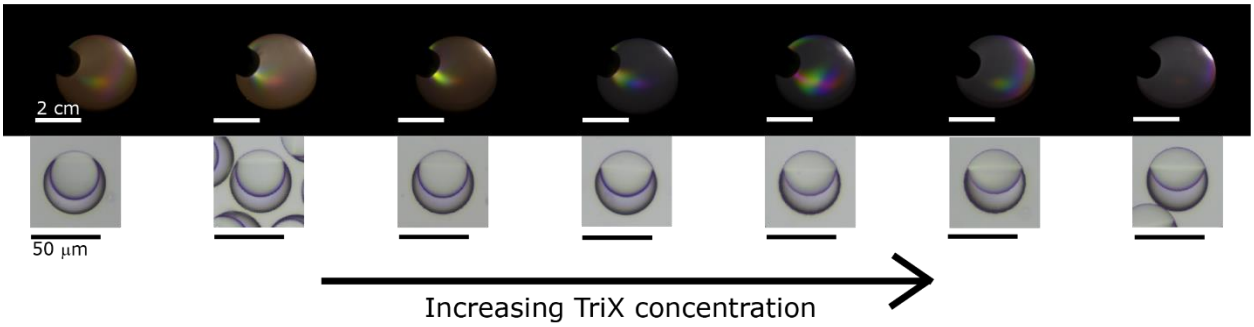

Figure 2. Summary images of ping-pong ball projections accompanied by corresponding microscopic images of perfluorohexane and a 1:1 mixture of hexane and heptane by volume beginning in 0.175wt% Capstone and continuing with additions of Triton X. From left to right, the Cap:TriX weight percent ratio in aqueous solution decreases causing emulsion droplets to go from a fluorocarbon favored phase to a more hydrocarbon favored phase. This change in droplet shape resulted in changes in the colors projected onto a ping-pong ball hemisphere. Image analysis was conducted for droplet shapes ranging from a fluorocarbon favored phase (no TriX) to a fully Janus phase (12.5 Cap:TriX ratio), however coloration was observed in ping-pong ball projections where emulsion droplets were submerged in surfactant solutions with Cap:TriX ratios ranging from 35.0:1 to 20.5:1. Macroscopic imaging settings: LA – 50°, CA – 50°, LCA – 60°.

Images of ping pong ball projections were taken in series with additional amounts of added Triton X-100 in order to simulate the amylase transition period in sequential static images. Side by side projections may be seen above in Figure 2, where a band of color is visible between the Capstone to TriX weight ratio of 35:1 to 20.5:1. The band is seen to first appear in an area farthest away from the light source. The beginnings of coloration may be seen just as the hydrocarbon phase peeks out of the fluorocarbon shell, which is a more fluorocarbon favored shape than those modelled in Goodling et al.[3] The color band then sweeps towards the light source, and then back out away from the source until no coloration is visible. Changes in the position of the color band are associated with the change in the shape of the emulsion droplet by the three-way contact angle as expected given the findings in Goodling et al. In addition to this, the most vibrant coloration may be seen when the angle of light incidence matches the three-way contact angle. This may be due to a higher probability of incident light rays hitting the three-way contact point in a suitable manor for refection at that angle.

When emulsion droplets were placed in the enzyme active surfactant solution and exposed to α-amylase, the full color band sweeping motion is visible as the droplet shape changed continuously. The full sweeping motion may be viewed in Movie S1 which exhibits continuous footage of a ping pong ball projection over these emulsions. During the transition, as many as six distinct colors may be seen at any given time. This continuous sweeping motion poses more information about the total internal reflection mechanism for droplet coloration.

Models in Goodling et al. do not currently predict coloration at such a drastic and nearly spherical three-way contact shape. Thus, an updated system of modeling is needed to mathematically predict color patterns at more concave contact points. This additional range of coloration implies that droplets may be more sensitive than orginally documented and have an added area for detection in colorimetric sensing applications.

Color variation as a function of droplet size and illumination angle

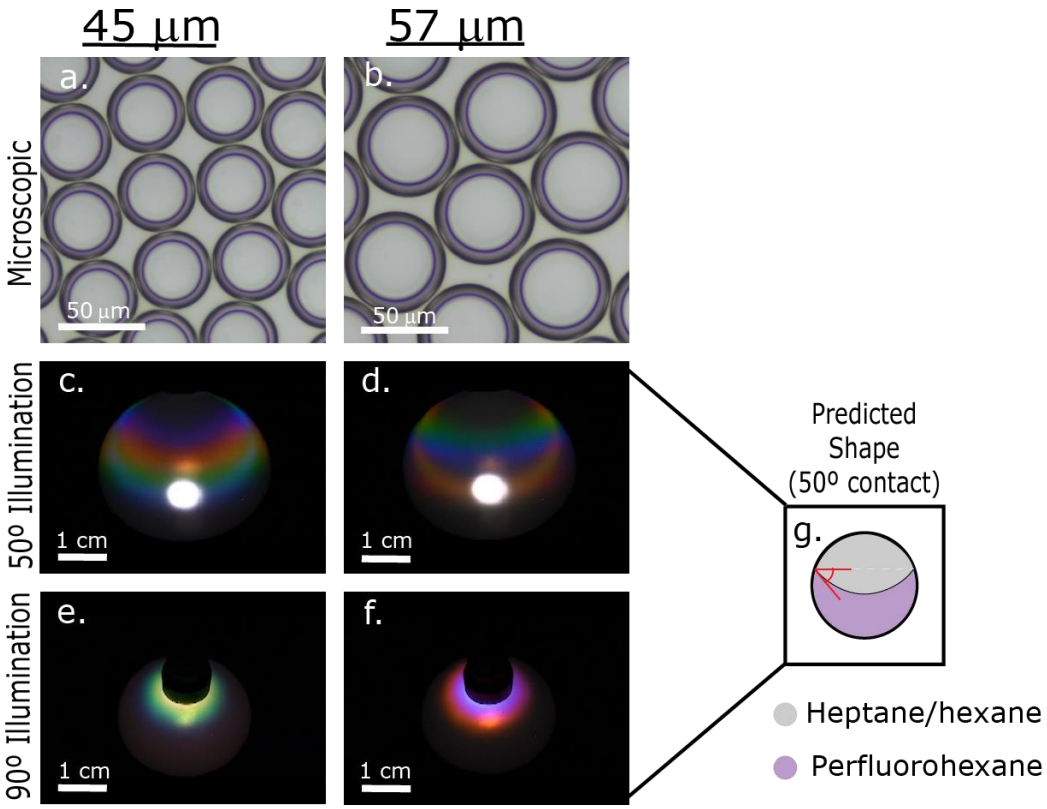

Figure 3. A comparison between droplets of two sizes and their influence of the color projections given off by the droplets. Images in the left-hand column correspond to emulsion droplets that are 45 microns in diameter, while images in the right-hand column correspond to droplets of a 57-micron diameter. Images a. - b. are microscopic top-down view images of PFH and 1:1 hexane/heptane by volume emulsion droplets submerged in 0.2 wt% Capstone in the two sizes specified. Images c. – d. are snapshots of ping-pong ball projections cast by emulsion droplets undergoing an amylase transition at its brightest state and with an IA of 50º. Images and e. – f. are also snapshots of ping-pong ball projections cast by emulsion droplets undergoing an amylase transitions. These images were taken during the same stage of the amylase transition to gain knowledge of color projections at the same droplet shape as images c. and d. at a different IA of 90º. Image g. is a sideview estimation of an emulsion droplet with similar shape to the predicted 50º three-way contact angle. This angle is believed to correspond to the brightest state of the amylase transition in images c. and d., and it is equivalent in measurement to the angle of illumination. Macroscopic imaging settings: CA – 50º, LCA – 60º.

In accordance with the results seen in Goodling et al., coloration varied by droplet size, even during the amylase transition. Figure 3 and Movie S2 show two samples that varied by sizes bordering 50 microns. Emulsion droplets in Figure 3a had a diameter of about 45 microns whereas droplets in Figure 3b had a diameter of about 57 microns. Figure 3c and 2d are snapshots of the amylase transitions of the corresponding samples in Movie S2 at their most vibrant state. Movie 2 shows the full side-by-side amylase transitions at a 50^o illumination angle where both samples undergo the same sweeping motion of the color band, however the color order of the band is modified based on the size of the emulsion droplets within the sample.

Angle dependence of color positions on light angle incidence is also expected, and was shown to be apparent in Movie S3, where changing the 50^o light incidence to 90^o incidence shows a different color pattern and a difference in the origins of the sweeping motion of the color band. As seen in Movie S3, at 90^o light incidence the color band originates and remains in a halo around the light source. This halo broadens and thins in a pulsing motion. Both samples exhibit instances when colors in the band do not form a full ring around the light source. This phenomenon may be due to concentration gradients of alpha-amylase in the surfactant solution and further action should be taken to maintain homogeneity in the sample. It was also noted that at a 90^o light angle incidence only a maximum of three distinct colors may be seen using the projection method.

The comparatively lower amount of colors visible and continuation of coloration around a single spot on the projection indicates that the 90^o illumination angle may be a better viewing angle for simplistic colorimetric sensing. At this angle, color changes are less variable, shorter in duration, and remain vibrant throughout most of the transition. These aspects make tracking simple vibrant colorimetric changes in one area easier for the price of less sensitivity. In using an emulsion system for enzyme activity detection, a clear starting and ending point of the amylase transition should be established. The beginnings of this application and implementation would benefit from the simplicity of recording the time between two distinct colors in the amylase transition, rather than tracking the band position in relation to the light source and color pattern within the band.

Phone imaging as a means of detection

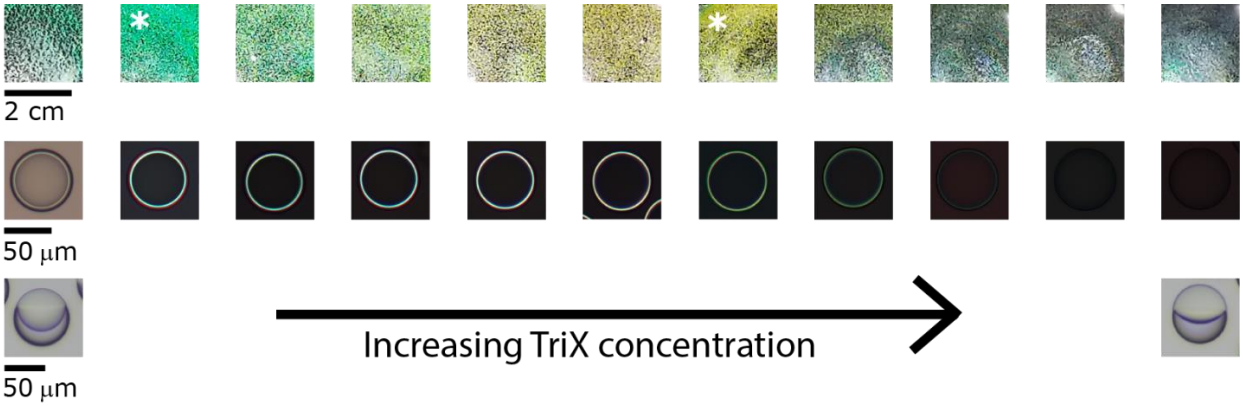

Figure 4. Images relating droplet shape of PFH and 1:1 Hep/hex drops to images see by phone and 10X magnification reflection microscope. Droplets began in 0.2 wt % Capstone and were introduced to higher concentrations of TriX from left to right and images in the same column correspond to the same droplet state (same size and shape). Top row images were captured by phone camera 18 inches above and parallel to the sample. This row displays the macroscopic effect of the emulsion droplets when imaged with phone flash in a light environment. Asterisk markers were placed on images with most saturated coloration and serve to mark suitable stages for the beginning and end points of amylase transition tracking. The middle row of microscopic images was collected via reflection microscope where vibrant coloration may be seen to radiate from the three-way contact ring of emulsion droplets. Coloration in this ring closely resembles coloration exhibited macroscopically in phone images in the top row. Bottom row images exhibit a microscopic sideview of emulsion droplets at the beginning and end of the TriX concentration range tested.

In response to viewing emulsion projections at 90^{o} incidence, phone images and videos were taken of the amylase transition and simulation with the phone flash serving as the illumination source. Static phone images were taken with the phone remaining parallel to the sample and compared to microscopic reflection and transmission images of the emulsion droplets, as seen in Figure 4. Coloration found in phone images closely match coloration of the three-way contact ring of emulsion droplets in the reflection microscope studied. This congruence indicates that both of these methods are equivalent in color detection possibilities. The direct imaging of the illuminated area in such a manner also allows for color information to be collected that would not otherwise be visible in the ping-pong ball projection, as the light source blocks this area in that method. A full amylase transition recorded by phone may be seen in Movie S4.

Phone and microscopic reflection imaging, when in focus at the center of the sample, usually yielded coloration limited to one color. This provides a more simplistic view for colorimetric sensing than the methods previously tested with ping-pong ball projections and opens pathways for comparatively easy computer automated color matching in regard to the other methods tested. This also method allows for amylase detection by recording the amount of time it takes for emulsion droplets to go from its most vibrant color state to another color.

These states, as an example are marked with asterisks in Figure 4 and correspond to a specific surfactant concentration of TriX and Capstone. Trials were expected to differ in color due to possible changes in droplet size and volume ratio in each droplet batch.[3] To combat this, each trial was calibrated by placing droplets in surfactant solutions of know concentration for the beginning and ending states to serve as a reference.

Controlled alpha amylase transition (from first instance of color to no color) times at room temperature (27 ^{o}C) ranged from 5 – 40 minutes in the 88 – 883 FAU/L range tested with time trials ranging from 2 – 18 minutes between calibrated color states. In order to further calibrate the limits of detection of the emulsion droplets, more time trials of the amylase enzyme should be conducted at 37 ^{o}C between activities from about 10 to 800 FAU/L in order to derive a continuous function for the relationship between enzyme activity and stage transition time. This is in accordance with body temperature and should increase the efficiency of the enzyme. Thus, trials will run more quickly, and less sample will be needed to achieve similar results.

Conclusion

A more comprehensive range of coloration in fluorocarbon/hydrocarbon emulsion droplets was explored via enzyme responsive surfactant solution. All findings in Goodling et al. were upheld with additional information found about the beginning stages of coloration in perfluorohexane and 1:1 hexane/heptane by volume droplets. Future studies should work to continuously correlate droplet shape with color band position by performing more detailed static image analysis at smaller changing increments in Triton X-100 and Capstone FS-30 ratios. Straight-on 90^{o} illumination offers less color sensitivity than glancing 50^{o} illumination angles, with three colors being projected during the amylase transition at 90^{o} illumination when compared to a maximum of 6 colors at 50^{o} illumination. This position of illumination while using a phone flash and camera allows for the beginnings of simple α-amylase detection via colorimetric calibration. Alpha-amylase activity ranging from 88 – 883 FAU/L were detected at stage transition times ranging from 2 – 18 minutes. Future studies should be conducted to determine the limits of detection of the emulsion droplet system. This may be done by performing more time trials to gain better knowledge of amylase activity and stage transition time dependence for field testing applications.

Supplemental Information

Supplementary images and all videos may be found in a Box folder found at the url: https://psu.app.box.com/folder/84795564653. All video descriptions and parameters may be found below.

Movie S1. Ping-pong ball projection of perfluorohexane and 1:1 heptane/hexane emulsion droplets after alpha-amylase was added to the drops in CTγ aqueous solution. Light incidence: 50º Camera angle: 50º Light-to-camera angle: 90º Video duration: 07 mins 06 secs at 25x speed.

Movie S2. Side by side view of ping-pong ball projections of perfluorohexane and 1:1 heptane/hexane emulsion droplets after alpha-amylase was added to the drops in CTγ aqueous solution. Light incidence: 45º Camera angle: 65º Light-to-camera angle: 180º Video durations: 07 mins 30 secs at 25x speed Left: Droplets in sample are 45 µm in size Right: Droplets in sample are 57 µm in size.

Movie S3. Side by side view of ping-pong ball projections of perfluorohexane and 1:1 heptane/hexane emulsion droplets after alpha-amylase was added to the drops in CTγ aqueous solution. Light incidence: 90º Camera angle: 65º Light-to-camera angle: 180º Video durations: 07 mins 30 secs at 25x speed. Left: Droplets in sample are 45 µm in size Right: Droplets in sample are 57 µm in size.

Movie S4. Phone video of perfluorohexane and 1:1 heptane/hexane emulsion droplets after alpha-amylase was added to the drops in CTγ aqueous solution. Phone angle: 90o Phone Height: 5 inches above sample Video Duration: 05 mins 30 secs at 30x speed.

References

(1) Zi, J.; Yu, X.; Li, Y.; Hu, X.; Xu, C.; Wang, X.; Liu, X.; Fu, R. **2003**, *100* (22).

(2) Luo, Z.; Evans, B. A.; Chang, C. **2019**.

(3) Goodling, A. E.; Nagelberg, S.; Kaehr, B.; Meredith, C. H.; Cheon, S. I.; Saunders, A. P.; Kolle, M.; Zarzar, L. D. *Nature* **2019**, *566* (7745).

(4) Zarzar, L. D.; Sresht, V.; Sletten, E. M.; Kalow, J. A.; Blankschtein, D.; Swager, T. M. *Nature* **2015**, *518* (7540), 520–524.

(5) Zarzar, L. D.; Kalow, J. A.; He, X.; Walish, J. J.; Swager, T. M. **2017**, *114* (15), 3821–3825.

(6) Saito, Y.; Ueda, H.; Abe, M.; Sato, T.; Christian, S. D. *Colloids Surfaces A* **1998**, *135*, 103–108.

(7) Nater, U. M.; Rohleder, N.; Gaab, J.; Berger, S.; Jud, A.; Kirschbaum, C.; Ehlert, U. *Int. J. Psychophysiol.* **2005**, *55* (3), 333–342.

(8) Chatterton, R. T.; Vogelsong, K. M.; Lu, Y.; Ellman, A. B.; Hudgens, G. A. *Clin. Physiol.* **1996**, 433–448.

(9) Vege, Santhi Swaroop; Chari, Suresh T ; Clain, J. E. *J. Am. Med. Assoc.* **2004**, *291* (23), 2865–2868.

(10) Kroll, M. *Clin. Chem.* **1999**.